

The global meter-level shape model of comet 67P/Churyumov-Gerasimenko

Frank Preusker, F. Scholten, K.-D. Matz, T. Roatsch, S. F. Hviid, S. Mottola, Jörg Knollenberg, Ekkehard Kührt, Maurizio Pajola, Nilda Oklay, et al.

▶ **To cite this version:**

Frank Preusker, F. Scholten, K.-D. Matz, T. Roatsch, S. F. Hviid, et al.. The global meter-level shape model of comet 67P/Churyumov-Gerasimenko. Astronomy and Astrophysics - A&A, 2017, 607 (November), L1 (5 p.). 10.1051/0004-6361/201731798 . insu-01631548

HAL Id: insu-01631548

https://insu.hal.science/insu-01631548

Submitted on 11 Nov 2020

HAL is a multi-disciplinary open access archive for the deposit and dissemination of scientific research documents, whether they are published or not. The documents may come from teaching and research institutions in France or abroad, or from public or private research centers.

L'archive ouverte pluridisciplinaire **HAL**, est destinée au dépôt et à la diffusion de documents scientifiques de niveau recherche, publiés ou non, émanant des établissements d'enseignement et de recherche français ou étrangers, des laboratoires publics ou privés.

A&A 607, L1 (2017)
DOI: 10.1051/0004-6361/201731798
© ESO 2017

Astronomy & Astrophysics

Letter to the Editor

The global meter-level shape model of comet 67P/Churyumov-Gerasimenko

F. Preusker[1], F. Scholten[1], K.-D. Matz[1], T. Roatsch[1], S. F. Hviid[1], S. Mottola[1], J. Knollenberg[1], E. Kührt[1], M. Pajola[2], N. Oklay[1], J.-B. Vincent[1], B. Davidsson[3], M. F. A'Hearn[4], J. Agarwal[5], C. Barbieri[6], M. A. Barucci[7], J.-L. Bertaux[8], I. Bertini[9], G. Cremonese[10], V. Da Deppo[11], S. Debei[12], M. De Cecco[13], S. Fornasier[7], M. Fulle[14], O. Groussin[15], P. J. Gutiérrez[16], C. Güttler[5], W-H. Ip[17,18], L. Jorda[15], H. U. Keller[1,19], D. Koschny[20], J. R. Kramm[5], M. Küppers[21], P. Lamy[15], L. M. Lara[16], M. Lazzarin[6], J. J. Lopez Moreno[16], F. Marzari[6], M. Massironi[9], G. Naletto[9,11,22], H. Rickman[3,23], R. Rodrigo[24,25], H. Sierks[5], N. Thomas[26,27], and C. Tubiana[5]

(Affiliations can be found after the references)

Received 18 August 2017 / Accepted 23 September 2017

ABSTRACT

We performed a stereo-photogrammetric (SPG) analysis of more than 1500 Rosetta/OSIRIS NAC images of comet 67P/Churyumov-Gerasimenko (67P). The images with pixel scales in the range 0.2−3.0 m/pixel were acquired between August 2014 and February 2016. We finally derived a global high-resolution 3D description of 67P's surface, the SPG SHAP7 shape model. It consists of about 44 million facets (1−1.5 m horizontal sampling) and a typical vertical accuracy at the decimeter scale. Although some images were taken after perihelion, the SPG SHAP7 shape model can be considered a pre-perihelion description and replaces the previous SPG SHAP4S shape model. From the new shape model, some measures for 67P with very low 3σ uncertainties can be retrieved: 18.56 km^3 ± 0.02 km^3 for the volume and 537.8 kg/m^3 ± 0.7 kg/m^3 for the mean density assuming a mass value of 9.982×10^{12} kg.

Key words. methods: data analysis – techniques: image processing – comets: individual: 67P/Churyumov-Gerasimenko – planets and satellites: surfaces

1. Introduction

For the precise mapping of a planetary body, and for other detailed analyses within various scientific investigations, a 3D shape model at the highest possible level of detail, accuracy, and completeness is a fundamental prerequisite. This is particularly important if the observed body is as irregular and bilobed as the nucleus of 67P/Churyumov-Gerasimenko (67P), the primary target of ESA's Rosetta mission. There are low-resolution global shape models of 67P from Earth-based telescope observations (e.g., Lowry et al. 2012) and from Rosetta approach images (Mottola et al. 2014) of the Optical, Spectroscopic, and Infrared Remote Imaging System (OSIRIS; Keller et al. 2007; Sierks et al. 2015). The first shape model that describes 67P in detail was published as SPG SHAP4S in Preusker et al. (2015) and was released as CG-DLR_SPG-SHAP4S-V1.0 on the europlanet website[1]. This model is based on DLR's stereo-photogrammetric analysis technique (SPG) and uses OSIRIS NAC image data that were acquired from early August to early September 2014. The model includes 218 OSIRIS NAC images with scales from 0.9 to 2.4 m/pixel. Since the observation period covered the northern summer, areas south of −20° latitude are not well illuminated and the shape model is therefore widely interpolated in southern regions. Jorda et al. (2016) applied another technique, the stereo-photoclinometric method (SPC) to more than 5500 OSIRIS NAC images (acquired through June 2015). Additional information from scans of the MIRO microwave instrument on board Rosetta were included in order to further constrain the topography of the southern hemisphere. The result, the SPC SHAP5 shape model (dataset name CG-SPC-SHAP5-V1.1) of 67P, benefits from its better coverage in the southern hemisphere, but compared to the SPG SHAP4S shape model it is evidently limited in its level of detail and its accuracy on the local and regional scale (see Fig. 1). For precise studies of 67P, it is essential to have a detailed 3D model of the entire surface. We decided to extend the 3D coverage of 67P to its southern hemisphere with the same level of

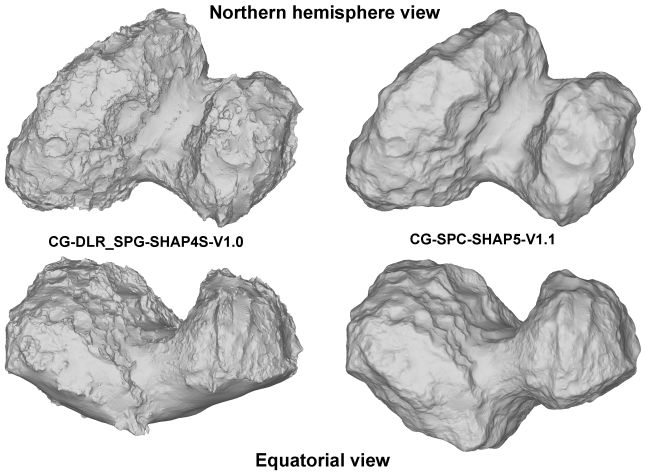


Fig. 1. Published Rosetta/OSIRIS shape models for 67P: *left*: SPG-based shape model (SPG SHAP4S, Preusker et al. 2015). *Right*: SPC-based shape model (SPC SHAP5, Jorda et al. 2016).

[1] http://europlanet.dlr.de/Rosetta

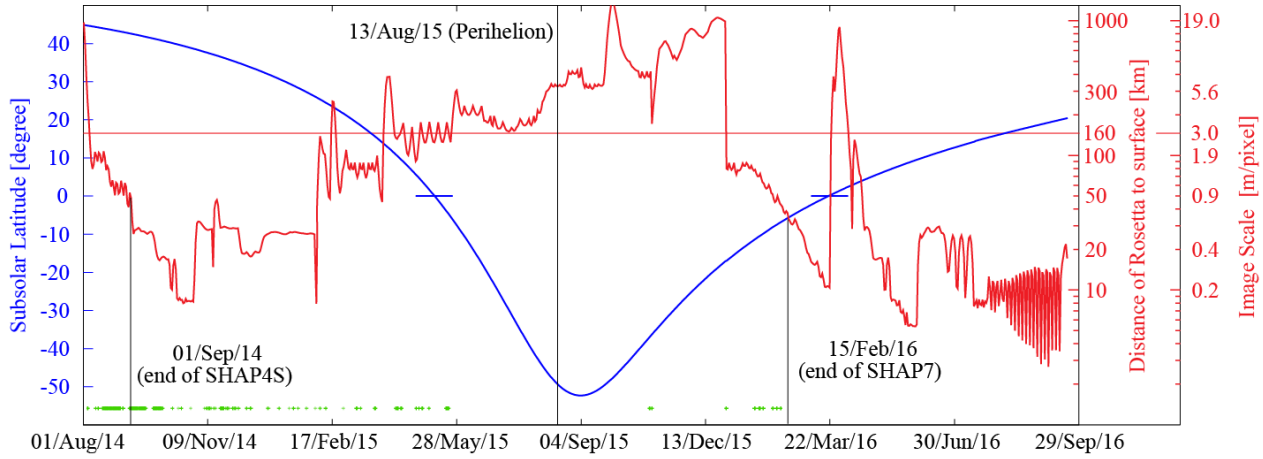


Fig. 2. Timeline of observation and illumination conditions during the Rosetta mission at 67P. Subsolar latitude (in blue), distance of the Rosetta s/c to the surface of 67P and corresponding OSIRIS NAC image scale (both in red), key dates (in black).

detail and accuracy that our previous SPG SHAP4S shape model provides for the northern hemisphere. Due to the morphological changes of 67P close to its perihelion passage, we also decided to aim for the reconstruction of 67P's global shape as it appeared prior to its perihelion on 13 August 2015. Therefore, it should be preferably based on pre-perihelion OSIRIS NAC images. Within this investigation we used the same method as for the derivation of the SPG SHAP4S model. The SPG approach has proven its efficiency and the quality of its results (2.5D Digital Terrain Models and 3D shape models) within many planetary missions over the past decades. During the Rosetta mission, we were finally able to prove SPG's universal applicability, even under extreme conditions, i.e., the very irregular shape of the nucleus of comet 67P with its large concavities. The following description may therefore be understood as a direct follow-up work of Preusker et al. (2015) where we described the SPG procedures and relevant aspects of the Rosetta mission and of comet 67P in great detail. Hence, this letter concentrates briefly on the extended OSIRIS NAC images dataset, on specific side-conditions for this SPG processing, and finally on the description of the new global 67P shape model that is dedicated to replacing the previous SPG SHAP4S shape model.

2. OSIRIS NAC image selection

The previous SPG SHAP4S shape model covers about 70 percent of the surface of 67P, i.e., the entire northern hemisphere and moderate southern latitudes. For the successful extension of the existing SPG shape model towards a real complete model we need an adequate set of additional OSIRIS images that cover higher southern latitudes. However, if we consider the very short time period previously used (5 August–3 September 2014), there may also be additional observations that allow improvements in already covered regions. The observation and illumination conditions during the Rosetta mission at 67P vary strongly over time. Figure 2 displays some of the key parameters that help to select adequate mission and observation phases for the final image data subset. Ideally, the desired shape model should be highly resolved and complete in terms of coverage. Therefore, and similarly to the SPG SHAP4S shape model, we decided to select 3 m/pixel as an upper limit for the image scale and to use high-resolution OSIRIS NAC images only. Following these criteria, the period that we initially selected starts on 5 August 2014 and lasts until 24 May 2015. It includes OSIRIS image sequences that were already used for the SPG SHAP4S shape model and additional sequences dedicated to 3D shape reconstruction. Several images from other OSIRIS mapping sequences during this time period complement the entire used OSIRIS NAC selection for a total of 1198 images. The subsolar latitude at the end of May 2015 is close to the equator, at about 6° S. For this reason, and because of 67P's very irregular shape, there are still some areas at high southern latitudes that suffer from typically low Sun elevation, and results in slighty increased point spacing in the final shape model at about 10% of the entire surface of 67P. Other southern summer pre-perihelion periods, e.g., in July 2015, with image scales only slightly higher than 3 m/pixel suffer from observational conditions that are not suitable for our analysis. For operational reasons (to guarantee the mission safety), the orbit of the Rosetta spacecraft was almost perpendicular to the Sun-comet direction so that images taken at that time suffer from high phase angles (up to 90°). This orbit strategy was followed over almost the entire Rosetta mission with few exceptions and is generally a limiting factor to the availability of adequate image content for many scientific applications. Appropriate OSIRIS NAC images at scales of 0.8 to 1.4 m/pixel and with sufficient illumination (phase angles $\ll 90°$ and subsolar latitudes in the south) were acquired in the first weeks of 2016. After this period, the phase angle again begins to rapidly increase to 90°. For a full global coverage, we decided to include 309 OSIRIS NAC images from this post-perihelion period. Finally, we filled a very small remaining gap in 67P's southern neck region with 24 images that were taken in October and November 2015. Table 1 summarizes information about the selected 1531 OSIRIS NAC images for the subsequent SPG processing (image times are marked in green in Fig. 2). We only selected images that were acquired with the OSIRIS NAC orange filter F22 (central wavelength: 649.2 nm, bandwidth: 84.5 nm) because of its high signal-to-noise ratio (Keller et al. 2007).

3. Stereo-photogrammetric processing towards the SPG SHAP7 shape model

The previously described dataset of more than 1500 OSIRIS NAC images constitutes the input for the subsequent stereo-photogrammetric processing. The latest images are from the OSIRIS SHAP7 image sequence, thus the new shape model is called SPG SHAP7. The major aspects of the SPG procedure are 1) the selection of sets of stereo images (stereo models) within

Table 1. Selection of OSIRIS NAC images for the generation of the SPG SHAP7 shape model.

Observation period	Count of images	Avarage image scale [m/pixel]	Subsolar latitude
2014-08-05–2014-09-03	281	1.1–2.1	43°N–45°N
2014-09-05–2014-09-23	336	0.5–0.8	41°N–43°N
2014-09-29–2015-02-14	359	0.2–0.5	24°N–40°N
2015-03-10–2015-03-25	31	1.5–1.6	15°N–19°N
2015-04-11–2015-04-15	191	2.4–2.7	5°S–10°N
2015-10-31–2015-11-02	24	5.2	36°S
2015-12-31–2016-01-01	16	1.4	16°S–17°S
2016-01-23–2016-02-13	293	1.1	6°S–11°S

the observation periods and a set of connecting stereo models between the periods, 2) the stereo image matching within and between these models, and 3) the overall stereo-photogrammetric block adjustment for the derivation of adjusted orientation data (orbit position and pointing) for each image, considering the body's rotational state. The 3D object point and 3D mesh generation are described in Sect. 4.

3.1. Setup of stereo models

Compared to the SPG SHAP4S model (derived from less than 300 images acquired within a month), the major difference of the input data for the SPG SHAP7 shape model is its size and diversity (more than 1500 images that were taken over more than 18 months). Within each single observation period, we defined stereo models for each image, i.e., combinations of the respective image and of at least two stereo partners that fulfill the typical observation and illumination requirements. We defined additional stereo models that serve as connectors between the single groups of stereo models within each observation period. In total, we defined a block of more than 4100 connected stereo models for the entire SPG SHAP7 shape model.

3.2. Stereo image matching

For each of the defined stereo models, we use SPG's area-based image matching technique (Wewel 1996) to derive image coordinates of identical points with the images. First, image matching is done in a more sparse way for the generation of a reduced set of tie-points that serves as input for the subsequent stereo-photogrammetric block adjustment. Later on, for the derivation of points for the 3D model itself, this grid is typically as dense as the original pixel size of the respective images. The reduced set of tie-points for the block adjustment comprises more than 20 000 points. The total number of points for the final SPG SHAP7 shape generation is about 6 billion.

3.3. Improvement of orientation data by means of stereo-photogrammetric block adjustment

Based on the reduced set of tie-points, we used a stereo-photogrammetric block adjustment that consists of a least-squares adjustment of observations (image coordinates of the tie-points) within (multi-)stereo images (i.e., the stereo models), in order to determine improved orientation data (spacecraft position and attitude) in the body-fixed coordinate frame from the initial set of orientation data. The typical initial or a priori set of orientation data consists of SPICE kernels (Acton 1996) and includes nominal SPICE SP orbit kernels, defined in the J2000 reference frame, for 67P and for the Rosetta spacecraft position, as well as nominal SPICE C kernels about the spacecraft attitude (pointing). The orientation of the body-fixed coordinate frame in the J2000 frame (i.e., the rotation model) is typically described by a SPICE PC kernel that describes planetary constants, e.g., the body's pole orientation, a possible precession, and the rotation period. For a pre-perihelion period from August to early September 2014, we detected a precession-like complex rotation for 67P which is described in a SPICE PC kernel (Preusker et al. 2015). This kernel also defines 67P's "Cheops" reference frame. The effect of the precession amounts to about ±3 m on 67P's surface. Later, the presence of this precession was confirmed by Gutiérrez et al. (2016) and Jorda et al. (2016). Additionally, a significant change from a constant to a varying rotation period, starting in late 2014 and caused by effects from sublimation activity, had been predicted early in the mission by Keller et al. (2015) based on the SPG SHAP4S shape model. This change in the rotation period of 67P was confirmed later within different analyses of image data that were taken around the comet's perihelion (e.g., Jorda et al. 2016). SPICE C kernels that describe this varying rotation of 67P's body-fixed frame in the J2000 frame are included in ESA's set of relevant Rosetta kernels[2]. These kernels define the state and orientation of the coordinate frames of 67P, of the Rosetta spacecraft, and of the instruments on board Rosetta over the entire mission. These kernels were used (with one exception) for the transformation of initial values for the orientation data to the coordinate frame of the SPG SHAP7 block adjustment, 67P's body-fixed frame 67P/C-G_CK. The exception is represented by the set of already existing adjusted orientation data for OSIRIS NAC images of the previous SPG SHAP4S processing. Since it considered the comet's pre-perihelion precession, we used orientation results from this previous adjustment as initial values within the SPG SHAP7 block adjustment, widely minimizing the possible influence of a systematic effect (the SPICE C kernels for 67P unfortunately do not contain the previously mentioned precession).

4. Final SPG SHAP7 shape model

Based on the adjusted orientation data and considering the image distortion model, we computed a 3D forward ray intersection for 6 billion matched points coordinates. The result is a set of 3D points in the body-fixed Cheops reference frame 67P/C-G_CK. Because of the redundancy from an intersection of three or more rays, we estimated additionally the intersection accuracy of each point. Secondly, we eliminated points that were derived from less than three stereo partners. We also eliminated outliers, i.e., points with a 3D intersection error that is larger than three times the mean intersection error within the respective stereo model. The remaining 3.4 billion points provide a mean 3D intersection accuracy of 0.3 m, which is representative of the mean accuracy of the final shape model. These points were then filtered by averaging points that fell within voxels of 1 m in size. We finally derived a meshed dataset using the Poisson surface reconstruction functionality in version 1.3.3 of the mesh processing system MeshLab© (Cignoni et al. 2008). Henceforth, we adopt the "vertex" for a 3D point and "facet" for a triangular mesh of three vertices. The final meshed SPG SHAP7 shape model consists

[2] ftp://ssols01.esac.esa.int/pub/data/SPICE/ROSETTA/kernels/mk

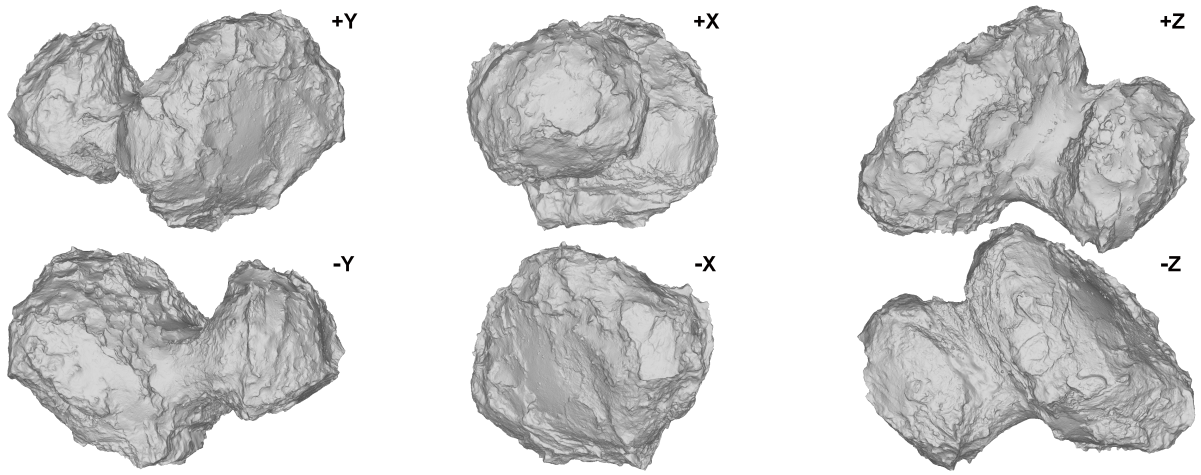


Fig. 3. Orthographic views of the SPG SHAP7 model along the primary axes of the body-fixed 67P/C-G_CK coordinate frame (indicated axes point towards the viewer, north is up for the +/−*XY* views, +*Y* is up for the +/−*Z* views).

Table 2. Shape model parameters and derived geometric measures for 67P including 3σ uncertainties.

Shape model	OSIRIS NAC images count	Number of final vertices/facets [Mio]	Average spacing [m]	Total volume [km^3]	Mean bulk density [kg/m^3]	Total surface area [km^2]
SPG SHAP4S (Preusker et al. 2015)	218	8.4/16.7	2.0	18.7 ± 0.2	534 ± 6	n/a
SPC SHAP5 (Jorda et al. 2016)	>5500	1.6/ 3.1	5.5	18.8 ± 0.9	532 ± 21	46.9 ± 7.5
SPG SHAP7 (this letter)	1531	22.0/44.0	1.0–1.5	**18.56 ± 0.02**	**537.8 ± 0.7**	**51.7 ± 0.1**

of 22 million vertices and 44 million facets. The technical name for this version of the SPG SHAP7 shape model is CG-DLR_SPG-SHAP7-V1.0. Figure 3 shows six different views of the new model. Details about the SPG SHAP7 shape model and some characteristic key parameters derived from this model are listed in Table 2. For comparison, we added the respective parameters for the SPG SHAP4S model and the SPC SHAP5 model. For the derivation of 67P's mass, we used the volume of $(9.982 \pm 3) \times 10^{12}$ kg from Pätzold et al. (2016). For compatibility within Table 2, we transformed 1σ uncertainties from Jorda et al. (2016) to 3σ estimates and finally reduced the uncertainties for the volume and bulk density measures from Preusker et al. (2015) since their assumed high uncertainty of 67P's center of mass was not confirmed later. We also derived various representations with a reduced number of facets – more adequate for some scientific applications – by applying the quadratic edge collapse decimation function in MeshLab©. The final dataset is available at the europlanet website[1].

5. Summary and outlook

Earlier analyses used OSIRIS NAC data for the derivation of the SPG-based shape model (SPG SHAP4S, Preusker et al. 2015) which provided detailed 3D information for about 70% of the surface of comet 67P, mainly on the northern hemisphere. With integrated additional OSIRIS NAC images from September 2014 to February 2016, we now present the SPG SHAP7 shape model, describing the entire surface of comet 67P with meter-scale lateral spacing and vertical accuracy typically of a few decimeters. We also achieved local improvements in low northern latitudes, based on observation phases in late 2014. Although some post-perihelion stereo images from the SHAP7 image sequence from early 2016 have been used to fill small gaps at high southern latitudes, the SPG SHAP7 shape model can be essentially considered a complete description of the pre-perihelion status of the surface of comet 67P's nucleus. Nevertheless, the image dataset spreads over more than 18 months. Therefore, we recommend that any study of local/regional surface changes along with 67P's perihelion passage must be performed with care and would probably work better with special subproducts of this global model. We plan to improve our model further, on both a global and local scale, by including results from pending investigations of the rotational state of 67P, particularly of the development of its known pre-perihelion precession until the end of the Rosetta mission in September 2016.

Acknowledgements. OSIRIS was built by a consortium of the Max-Planck-Institut für Sonnensystemforschung, Göttingen, Germany, CISAS – University of Padova, Italy, the Laboratoire d'Astrophysique de Marseille, France, the Instituto de Astrofísica de Andalucia, CSIC, Granada, Spain, the Research and Scientific Support Department of the European Space Agency, Noordwijk, The Netherlands, the Instituto Nacional de Técnica Aeroespacial, Madrid, Spain, the Universidad Politéchnica de Madrid, Spain, the Department of Physics and Astronomy of Uppsala University, Sweden, and the Institut für Datentechnik und Kommunikationsnetze der Technischen Universität Braunschweig, Germany. The support of the national funding agencies of Germany (DLR), France (CNES), Italy (ASI), Spain (MEC), Sweden (SNSB), and the ESA Technical Directorate is gratefully acknowledged. This work has also received funding from the European Union's Horizon 2020 research and innovation programme under grant agreement No. 686709 (MiARD).

References

Acton, C. H. 1996, Planet. Space Sci., 44, 65
Cignoni, P., Callieri, M., Corsini, M., et al. 2008, in Eurographics Italian Chapter Conference 2008, Salerno, Italy, 129
Gutiérrez, P. J., Jorda, L., Gaskell, R. W., et al. 2016, A&A, 590, A46
Jorda, L., Gaskell, R., Capanna, C., et al. 2016, Icarus, 277, 257
Keller, H. U., Barbieri, C., Lamy, P., et al. 2007, Space Sci. Rev., 128, 433
Keller, H. U., Mottola, S., Skorov, Y., & Jorda, L. 2015, A&A, 579, L5

Lowry, S., Duddy, S. R., Rozitis, B., et al. 2012, A&A, 548, A12
Mottola, S., Lowry, S., Snodgrass, C., et al. 2014, A&A, 569, L2
Pätzold, M., Andert, T., Hahn, M., et al. 2016, Nature, 530, 63
Preusker, F., Scholten, F., Matz, K.-D., et al. 2015, A&A, 583, A33
Sierks, H., Barbieri, C., Lamy, P. L., et al. 2015, Science, 347
Wewel, F. 1996, Int. Arch. Photogram. Remote Sensing, 31, 936

[1] German Aerospace Center (DLR), Institute of Planetary Research, 12489 Berlin, Germany
e-mail: Frank.Preusker@dlr.de
[2] NASA Ames Research Center, Moffett Field, CA 94035, USA
[3] Department of Physics and Astronomy, Uppsala University, Box 516, 75120 Uppsala, Sweden
[4] University of Maryland, Department of Astronomy, College Park, MD 20742-2421, USA
[5] Max Planck Institute for Solar System Research, Justus-von-Liebig-Weg 3, 37077 Göttingen, Germany
[6] University of Padova, Department of Physics and Astronomy, Vicolo dell'Osservatorio 3, 35122 Padova, Italy
[7] LESIA, Observatoire de Paris, PSL Research University, CNRS, Univ. Paris Diderot, Sorbonne Paris Cité, UPMC Univ. Paris 06, Sorbonne Universités, 5 place Jules Janssen, 92195 Meudon, France
[8] LATMOS, CNRS/UVSQ/IPSL, 11 boulevard d'Alembert, 78280 Guyancourt, France
[9] Center of Studies and Activities for Space (CISAS) "G. Colombo", University of Padova, via Venezia 15, 35131 Padova, Italy
[10] INAF–Osservatorio Astronomico di Padova, Vicolo dell'Osservatorio 5, 35122 Padova, Italy
[11] CNR – IFN UOS Padova LUXOR, via Trasea 7, 35131 Padova, Italy
[12] Department of Industrial Engineering, University of Padova, via Venezia 1, 35131 Padova, Italy
[13] University of Trento, Faculty of Engineering, via Mesiano 77, 38121 Trento, Italy
[14] INAF–Osservatorio Astronomico di Trieste, via Tiepolo 11, 34143 Trieste, Italy
[15] Aix-Marseille Université, CNRS, LAM (Laboratoire d'Astrophysique de Marseille), UMR 7326, 38 rue Frédéric Joliot-Curie, 13388 Marseille, France
[16] Instituto de Astrofísica de Andalucía (CSIC), c/ Glorieta de la Astronomìa s/n, 18008 Granada, Spain
[17] Graduate Institute of Astronomy, National Central University, 300 Chung-Da Rd, Chung-Li 32054, Taiwan
[18] Space Science Institute, Macau University of Science and Technology, Avenida Wai Long, Taipa, Macau, PR China
[19] Institut für Geophysik und extraterrestrische Physik (IGEP), Technische Universität 31 Braunschweig, Mendelssohnstr. 3, 38106 Braunschweig, Germany
[20] Scientific Support Office, European Space Research and Technology Centre/ESA, Keplerlaan 1, Postbus 299, 2201 AZ Noordwijk ZH, The Netherlands
[21] Operations Department, European Space Astronomy Centre/ESA, PO Box 78, 28691 Villanueva de la Cañada, Madrid, Spain
[22] Department of Information Engineering, University of Padova, via Gradenigo 6/B, 35131 Padova, Italy
[23] PAS Space Research Center, Bartycka 18A, 00716 Warszawa, Poland
[24] Centro de Astrobiología, CSIC-INTA, Torrejón de Ardoz, 28850 Madrid, Spain
[25] International Space Science Institute, Hallerstrasse 6, 3012 Bern, Switzerland
[26] Physikalisches Institut der Universität Bern, Sidlerstr. 5, 3012 Bern, Switzerland
[27] Center for Space and Habitability, University of Bern, 3012 Bern, Switzerland